**Coupled Systems Mechanics,** *Vol. 15, No. 2 (2026) 115-134*
https://doi.org/10.12989/csm.2026.15.2.115

Techno-Press

# Unsteady gas dynamics in relief-influenced pipelines: analytical modeling and pressure inversion

Ilgar G. Aliyev*

*Head of Operation and Reconstruction of Buildings and Facilities Department, Azerbaijan University Architecture and Construction, Baku, Azerbaijan*

*(Received July 28, 2025, Revised February 23, 2026, Accepted February 27, 2026)*

**Abstract.** This study presents a novel analytical framework for modeling unsteady gas flow in long-distance pipelines laid across nonuniform terrain. Unlike existing approaches that typically neglect gravitational and geometric complexities, the proposed model incorporates slope-dependent gravitational effects through exponential modulation coefficients and accounts for transient leakage using a time-dependent source term located at an arbitrary point along the pipeline. Using Charny's linearization method, the nonlinear governing equations are reduced to a solvable diffusion-type partial differential equation. A closed-form solution for pressure distribution P(x,t) is derived by applying a strategic substitution that separates terrain and friction effects, enabling Laplace-based inversion to yield physically interpretable results. The derived pressure expression reveals how leakage intensity ($G_{ut}$), terrain slope ($\alpha_1$), and leak location ($\ell$) interact to produce non-intuitive pressure patterns-such as pressure inversion, where downstream pressure loss becomes smaller than that at the inlet. The model is validated through extensive simulations, and key pressure dynamics are analyzed across multiple operating scenarios. Results indicate that increasing slope angle magnifies the gravitational effect, leading to early pressure crossover phenomena and stronger downstream stability, even for high leakage rates. This finding has substantial implications for sensor deployment, leak localization, and the development of SCADA-integrated decision-making tools. This work constitutes the first known analytical solution to the unsteady gas dynamics problem in sloped pipeline systems with leakage and provides a critical foundation for next-generation monitoring and control strategies in energy transport infrastructure.

**Keywords:** analytical model; Charny linearization; pressure inversion; relief-influenced pipelines; SCADA/IoT integration; unsteady gas flow

## 1. Introduction

The safe and efficient operation of gas transmission pipelines remains a critical issue in energy infrastructure management, particularly in geographically complex terrains. In accordance with engineering design standards for gas pipeline systems, the effect of terrain elevation must be accounted for when pipeline segments are located more than 100 meters above or below the inlet level. In such cases, gravitational forces and vertical pressure gradients significantly influence the unsteady flow behavior and pressure distribution along the pipeline. Neglecting the terrain-induced pressure variation can lead to inaccurate modeling, reduced operational efficiency, and potential safety risks, especially under variable demand or leakage scenarios. Unsteady gas dynamics

*Corresponding author, Associate Professor, E-mail: ilgar.aliyev1@azmiu.edu.az



ISSN: 2234-2184 (Print), 2234-2192 (Online)

modeling under leakage conditions has become essential for both early failure detection and reliability assessment in pipeline networks. Terrain-induced effects such as elevation change, gravitational forces, and frictional variations introduce additional complexity into the transient flow behavior of compressible fluids. Traditional models often assume uniform terrain or neglect slope-induced pressure alterations, which limits their applicability to real-world pipeline installations traversing mountainous regions. In such cases, leakage-induced pressure disturbances interact with terrain-driven gravitational effects, leading to asymmetric pressure profiles and unexpected propagation patterns.

This study proposes a novel analytical model for pressure distribution in sloped gas pipelines under unsteady flow conditions. The model incorporates gravitational effects through slope-dependent coefficients and captures leakage dynamics using a time-dependent source term. Numerical simulations are performed to evaluate pressure behavior at key pipeline segments, highlighting how leakage intensity and terrain inclination jointly affect system response. The results demonstrate new pressure inversion phenomena and provide valuable insights for sensor placement and SCADA-based monitoring.

## 2. Literature review and related work

The modeling of transient gas flow in pipelines has been extensively studied over the past decades. Foundational contributions by established early methodologies for simulating unsteady flow of compressible fluids [1]. In practical engineering applications, however, pipeline operation is still frequently evaluated using steady-state hydraulic formulations such as the, which provide reliable capacity estimates under stationary conditions [2, 3]. These relations assume quasi-uniform pressure gradients and therefore cannot represent the time-dependent redistribution of pressure caused by leakage or terrain-induced gravitational effects. In subsequent years, advancements have focused on parameter estimation techniques leveraging transient-state measurements for real-time leak detection [4-6].The influence of terrain topography on gas dynamics has gained increasing attention. For instance, conducted CFD-based analyses of unsteady leakage in mountainous pipelines with high-$H_2S$ content, highlighting pressure and dispersion asymmetry due to elevation changes [7, 8]. Similarly, developed a hierarchical physics-informed neural network to simulate hydraulic transients in complex topologies, aligning with SCADA/IoT system requirements for real-time diagnostics [10].

In parallel, emerging methodologies integrate machine learning for leak localization: applied a hybrid dynamic–ML model to improve classification accuracy under transient conditions, while achieved computational efficiency through physics-informed PINNs tailored to hydraulic systems [9, 10]. From a numerical modeling perspective, made advancements in finite difference and finite volume methods that consider elevation effects in pipelines [11, 12]. Engineering challenges such as liquid plug formation due to relief geometry were examined by and terrain-related construction complications addressed by [13, 14]. Despite these contributions, none offer closed-form analytical solutions that capture the combined effects of terrain slope, leakage location, and transient flow. The present study fills this gap by providing an analytical framework with explicit physical interpretation and numerical validation.

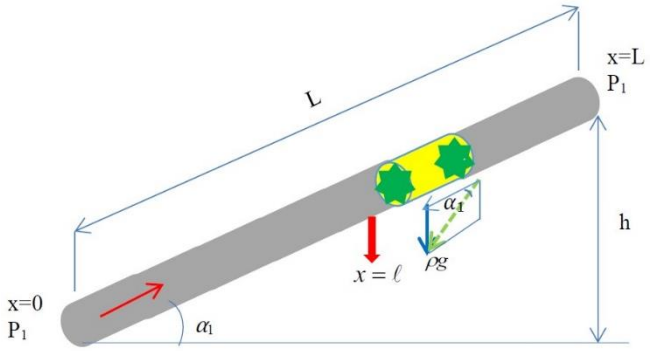


Figure 1. Schematic layout of a gas pipeline traversing a relief profile with internal leakage at position ℓ. The pipeline exhibits constant cross-section and is affected by gravity and friction along slope $\alpha_1$

## 3. Mathematical model

The dynamic behavior of gas flow in pipelines laid across uneven terrain presents a significant modeling challenge due to the combined effects of friction, gravitational forces, and local disturbances such as leakage. In this study, the pipeline is considered to exhibit a uniform cross-section but variable elevation, characterized by an inclination angle $\alpha_1$. A leakage is assumed to occur at a known location ℓ, and the gas is modeled under isothermal, compressible, and unsteady flow conditions (Fig. 1).

### 3.1 Governing equations

The flow behavior in a terrain-influenced gas pipeline is initially described by a system of nonlinear partial differential equations representing:
Mass conservation:

$$\frac{\partial \rho}{\partial t} + \frac{\partial (\rho v)}{\partial x} = -\delta (x - \ell) G_{ut} \tag{1}$$

Here $\delta(x-\ell)$ denotes the Dirac delta distribution representing a spatially localized leakage located at position $x=\ell$. The function $G_{ut}(t)$ describes the leakage intensity, i.e., the rate of mass loss converted into an equivalent pressure sink in the linearized gas-dynamic formulation. Its unit Pa×s/m follows from the reduction of the continuity–momentum system, where the leakage mass imbalance is expressed as a distributed pressure-loss term compatible with the Charny-type model. The leakage parameter $G_{ut}$ represents the equivalent pressure sink associated with mass loss. In practice it is determined from operational measurements. The imbalance between inlet and outlet flow rates provides the leakage mass rate, which is converted into the pressure source term through the linearized momentum relation. Therefore, the parameter is physically measurable and not an empirical fitting constant. For noisy data, a short-window least-squares adjustment between measured and predicted pressure traces may be applied to improve stability of the estimate.

Momentum conservation:

$$\frac{\partial (\rho v)}{\partial t} + \frac{\partial (\rho v^2)}{\partial x} + \frac{\partial P}{\partial x} + \lambda \frac{\rho v |v|}{2d} + \rho g \sin \alpha_1 = 0 \tag{2}$$

Here, ρ-is the gas density, v-is the flow velocity, P-is the pressure, d-is the pipe diameter, λ-is the hydraulic resistance coefficient, and g-is gravitational acceleration.

These equations are nonlinear and difficult to integrate directly. To make the system tractable, we employ I.A. Charny's linearization approach, which introduces an intermediate impulse element and simplifies the system into a form suitable for analytical manipulation.

### 3.2 Reduction of the governing hyperbolic system via charny linearization

The continuity and momentum equations form a nonlinear hyperbolic system describing compressible gas motion in pipelines. In its full form, this system supports acoustic wave propagation. However, in long transmission pipelines the frictional dissipation is sufficiently strong that high-frequency wave components decay rapidly and are not detectable at the operational monitoring time scale (SCADA scale: seconds to minutes). Consequently, the observable transient behavior corresponds to a slowly evolving pressure redistribution rather than oscillatory wave motion.

To obtain a tractable analytical formulation, the classical linearization proposed by I.A. Charny is applied. The key assumption of this approach is that, for slow transients, the convective acceleration term in the momentum equation is negligible compared to frictional resistance. The nonlinear term proportional to $\partial u/\partial x$ is therefore replaced by a linear resistance proportional to the flow rate. This converts the original hyperbolic system into a dissipative propagation model while preserving conservation of mass.

After linearization, the governing equations may be written schematically as

$$\frac{\partial P}{\partial t} + c^2 \frac{\partial G}{\partial x} = -c^2 G_{ut} \delta(x - \ell)$$

$$\frac{\partial P}{\partial x} + 2aG + \rho g \sin\alpha_1 = 0 \Rightarrow \frac{\partial G}{\partial x} = -\frac{1}{2a}\frac{\partial^2 P}{\partial x^2} - \frac{g}{2ac^2}\frac{\partial P}{\partial x}\sin\alpha_1$$

where P is pressure deviation and G is mass-flow rate. The coefficient $a=\lambda v/(2d)$ is the Charny linearization attenuation parameter [$s^{-1}$], representing frictional dissipation of momentum.

Differentiating the continuity equation with respect to time and substituting the linearized omentum relation eliminates the flow variable G. This yields a single partial differential equation expressed only in terms of pressure:

$$\frac{\partial^2 P}{\partial x^2} = \frac{2a}{c^2}\frac{\partial P}{\partial t} - \frac{\partial P}{\partial x}\frac{g}{c^2}\sin\alpha_1 + 2aG_{ut}\delta(x - \ell_2) \tag{3}$$

-$\lambda_1$ - friction-induced attenuation rate,

-$\lambda_2$ - gravity-induced drift parameter determined by the inclination angle $\alpha_1$.

Eq. (3) has a parabolic mathematical structure. It does not describe acoustic wave propagation; instead, it governs relaxation-type propagation of pressure disturbances under dominant friction. This behavior agrees with field observations in long pipelines, where oscillatory pressure waves decay rapidly and only monotonic transient pressure evolution remains measurable.

### 3.3 Boundary conditions and physical ınterpretation

To obtain an analytical solution, appropriate boundary conditions must be specified at the inlet x=0 and outlet x=L.

In the present study, the following zero-gradient conditions are adopted:

$$\left.\frac{\partial P(x,t)}{\partial x}\right|_{x=0} = \left.\frac{\partial P(x,t)}{\partial x}\right|_{x=L} = 0$$

These boundary conditions are adopted for a friction-dominated, SCADA-resolved transient where acoustic wave reflections are strongly damped; the model targets monotonic relaxation dynamics rather than high-frequency wave tracking. At first glance, such conditions may appear equivalent to imposing constant pressure boundaries.

However, their physical meaning in the present context is different. The model does not describe an acoustically driven wave propagation problem but rather the internal redistribution of pressure caused by leakage within a long pipeline segment over short operational time scales (tens to hundreds of seconds).

In real transmission systems, compressor stations and regulation valves do not instantaneously fix boundary pressure gradients; instead, they maintain slowly varying mass-flow conditions. Consequently, during the short transient interval following a leakage event, the internal pressure field evolves much faster than the external boundary control response.

Therefore, the pipeline segment may be treated as hydraulically quasi-isolated for the purpose of transient redistribution analysis. Under these circumstances, the zero-gradient boundary represents a reflective hydraulic boundary rather than a constant-pressure reservoir.

Physically, this means:

-no external pressure wave is injected from the boundaries,

-the transient disturbance is generated only by the internal leakage source,

-the system evolves toward a new equilibrium through dissipative redistribution.

This type of boundary specification is commonly used when deriving benchmark analytical solutions for long-pipeline transients dominated by frictional damping.

Because friction suppresses high-frequency acoustic oscillations, measurable SCADA data exhibit smoothed pressure relaxation rather than classical wave reflections.

The adopted boundary conditions therefore ensure mathematical solvability while remaining consistent with observed operational behavior.

Importantly, the model captures attenuated disturbance propagation, not ideal acoustic wave motion.

The pressure evolution is governed by diffusion-like damping combined with gravitational drift ($\lambda_2$), which redistributes pressure along the terrain slope even in the absence of boundary-imposed gradients.

The initial condition is assumed uniform:

$P(x,0)=P_1$ representing a steady operating regime prior to leakage occurrence.

The subsequent deviation from this state is fully driven by the localized sink term $G_{ut}(t)\delta(x-\ell)$.

The imposed zero-gradient boundary conditions do not represent fixed-pressure reservoirs. They approximate a quasi-isolated operational window in which boundary control actions are slower than internal leakage-driven redistribution. The resulting transient response therefore reflects attenuation- and slope-driven rebalancing rather than acoustic wave reflection.

### 3.4 Solution normalization via substitution

Eq. (3) contains first-order spatial drift and temporal attenuation terms.

These terms complicate the direct analytical solution and obscure the underlying operator

structure. Therefore, an exponential transformation is introduced to eliminate the first-order operators and reduce the equation to a canonical parabolic form suitable for solution by the Laplace transform and eigenfunction expansion.

Let

$$P(x,t) = U(x,t)e^{\lambda_1 t}e^{\lambda_2 x} \tag{4}$$

where the exponential factors are chosen to eliminate the linear attenuation and drift operators.

$$\frac{\partial P}{\partial t} = e^{\lambda_1 t+\lambda_2 x}\left(\frac{\partial U}{\partial t}+\lambda_1 U\right)$$

$$\frac{\partial P}{\partial x} = e^{\lambda_1 t+\lambda_2 x}\left(\frac{\partial U}{\partial x}+\lambda_2 U\right)$$

$$\frac{\partial^2 P}{\partial x^2} = e^{\lambda_1 t+\lambda_2 x}\left(\frac{\partial^2 U}{\partial x^2}+2\lambda_2\frac{\partial U}{\partial x}+\lambda_2^2 U\right)$$

Substituting these expressions into Eq. (3) and dividing by the common exponential factor $e^{\lambda_1 t+\lambda_2 x}$ yields

$$\frac{\partial U}{\partial t}+\lambda_1 U = \frac{2a}{c^2}\left(\frac{\partial^2 U}{\partial x^2}+2\lambda_2\frac{\partial U}{\partial x}+\lambda_2^2 U\right)-\lambda_2\left(\frac{\partial U}{\partial x}+\lambda_2 U\right)-$$
$$-\lambda_1 U+2aG_{ut}\delta(x-\ell)e^{-\lambda_1 t-\lambda_2 x}$$

After collecting terms, the coefficients multiplying U and ∂U/∂x cancel due to the specific choice of exponential transformation. The governing equation reduces to

$$\frac{\partial^2 U}{\partial X^2} = \frac{2a}{c^2}\frac{\partial U}{\partial t}+2aG_{ut}\delta(x-\ell_2)e^{-\lambda_1 t}e^{-\lambda_2 x} \tag{4a}$$

Here,

$$\lambda_1 = -\frac{g^2\,\mathrm{Sin}^2\,\alpha_1}{2a4c^2},\ \mathrm{s}^{-1} \qquad \lambda_2 = -\frac{g\,\mathrm{Sin}\,\alpha_1}{2c^2},\ \mathrm{m}^{-1}$$

Eq. (4a) is the canonical parabolic form of the original gas-dynamic problem.

The transformation removes drift and attenuation operators and isolates the intrinsic redistribution dynamics governed by the second-order spatial operator.

It should be emphasized that Eq. (4a) is not a physical diffusion equation describing molecular transport. The coefficient a=λv/(2d) introduced during Charny linearization represents friction-controlled attenuation of momentum, and the transformation converts the original damped hyperbolic system into a relaxation-propagation equation suitable for analytical treatment using Laplace transform and Green's function techniques.

Thus, the substitution (4) serves as a mathematical normalization that reveals the underlying dissipative pressure redistribution mechanism rather than altering the physics of the original system.

### 3.5 Analytical solution using laplace transform

Applying the Laplace transform to the linearized PDE yields a second-order ODE in the Laplace domain:

$$\frac{d^2U(x,s)}{dx^2} - \frac{2a}{c^2}sU(x,s) = 2aG_{ut}\delta(x-\ell_2)\frac{e^{-\lambda_2 x}}{s+\lambda_2} - \frac{2a}{c^2}P_1 e^{-\lambda_2 x} \tag{5}$$

Solving this and applying the inverse Laplace transform, we obtain the closed-form expression for the pressure distribution:

$$P_1(x,t) = P_1 - \frac{c^2 G_{ut}}{2L}e^{-\lambda_2(\ell-x)} \times \left[\frac{c^2\lambda_2^2}{2a\lambda_1}\left[t + \frac{e^{\lambda_1 t}-1}{\lambda_1}\right] + \left[\frac{\left(e^{-\lambda_1 t}-1\right)}{\lambda_1} + 2\sum_{n=1}^{\infty}\mathrm{Cos}\frac{\pi n(x-\ell)}{L}\frac{1-e^{-(\alpha-\lambda_1)t}}{\alpha-\lambda_1}\right] + \right.$$
$$\left. + \sum_{n=1}^{\infty}\mathrm{Cos}\frac{\pi n(x+\ell)}{L}\left[\frac{t}{\alpha-\lambda_1} - \frac{1-e^{-(\alpha-\lambda_1)t}}{(\alpha-\lambda_1)^2}\right]\cdot\left[\alpha + \frac{\pi n c^2\lambda_2}{2aL} - \frac{c^2\lambda_2^2}{2a}\right]\right] \tag{6}$$

where the remaining series terms represent eigenfunction expansions accounting for reflections and interactions at the leakage point.

List of Symbols Used in the Mathematical Model

For clarity and dimensional consistency, all symbols appearing in the reduced governing equation are summarized below.

| Symbol | Meaning | Unit |
|---|---|---|
| x | Spatial coordinate along the pipeline | m |
| t | Time | s |
| L | Pipeline length | m |
| d | Pipe diameter | m |
| P(x,t) | Gas pressure | Pa |
| U(x,t) | Transformed pressure function | Pa |
| G(x,t) | pressure-like flux variable (linearized momentum variable) | Pa×s/m |
| c | Isothermal speed of sound | m/s |
| λ | Darcy–Weisbach friction factor | – |
| v | Average gas velocity in steady state | m/s |
| a=λv/(2d) | Charny linearization attenuation parameter | $s^{-1}$ |
| $\lambda_1$ | Temporal attenuation coefficient | $s^{-1}$ |
| $\lambda_2$ | Spatial drift coefficient (terrain effect) | $m^{-1}$ |
| $\alpha_1$ | Pipeline inclination angle | rad (or deg) |
| g | Gravitational acceleration | $m/s^2$ |
| δ(x−ℓ) | Dirac delta distribution (leak location) | $m^{-1}$ |
| ℓ | Leak position | m |
| $G_{ut}(t)$ | Leakage intensity (equivalent pressure sink) | Pa×s/m |

## 4. Results and physical ınterpretation

The analytical expression derived in the previous section allows evaluation of the pressure

evolution along the pipeline for different leakage positions, terrain slopes, and leakage intensities. Instead of representing a propagating acoustic wave, the obtained solution describes a dissipative redistribution of pressure initiated by a localized disturbance. Immediately after leakage occurrence, the pressure field begins to reorganize spatially, and the disturbance spreads over the entire pipeline domain rather than forming a sharp moving front. This behavior follows directly from the dominance of frictional damping in long gas transmission lines.

At early times, the pressure deviation remains concentrated near the leakage point. However, as time progresses, the disturbance expands and interacts with the global hydraulic balance of the pipeline. The attenuation term governed by the parameter $\lambda_1$ reduces the magnitude of the disturbance, while the drift term $\lambda_2$ introduces a systematic bias in the direction of the terrain slope. Consequently, pressure redistribution becomes asymmetric even when the initial state is uniform.

A key feature revealed by the model is that the inlet and outlet pressures do not respond identically to leakage. For small inclination angles and low leakage intensity, the pressure decline remains nearly symmetric relative to the leak position. As either the slope or the leakage intensity increases, the downstream section becomes more sensitive to the disturbance. In such cases, the pressure drop at the pipeline outlet may exceed the pressure drop near the inlet, producing the pressure inversion phenomenon identified in this work.

This inversion does not contradict conservation laws. It results from the coupling of gravitational drift and distributed hydraulic resistance. The leakage reduces local mass flow, and the system compensates by redistributing pressure along the entire pipeline length. Because gravitational effects accumulate spatially, the downstream portion experiences a larger integrated resistance, leading to stronger pressure decay there even if the leak occurs upstream.

Another important observation is that the disturbance does not propagate as a classical wave. Instead, it relaxes toward a new equilibrium state through a diffusion-like process. The characteristic time scale of this relaxation depends primarily on the effective dissipation coefficient and only secondarily on the leak position. Therefore, long pipelines act as hydraulic filters, smoothing high-frequency variations and preserving only the large-scale transient signature detectable by monitoring systems.

The analytical solution also explains why leak detection based solely on local pressure gradients may fail in terrain-affected pipelines. Since the disturbance spreads globally, the diagnostic information is contained in the time evolution of pressure at multiple locations rather than in instantaneous spatial gradients. This observation supports the use of model-based identification rather than threshold-based detection.

Overall, the results demonstrate that leakage in relief-influenced pipelines produces a global transient redistribution rather than a localized wave phenomenon. The pressure inversion effect emerges naturally from the interaction between frictional dissipation and gravitational drift and therefore represents a physically consistent feature of long-distance gas transmission dynamics rather than a modeling artifact.

## 5. Engineering interpretation and diagnostic implications

While the analytical solution describes the mathematical evolution of pressure, its primary value lies in the engineering interpretation of transient behavior observed in real pipeline monitoring systems. The calculated pressure histories show that leakage does not manifest as a localized disturbance confined to the vicinity of the defect. Instead, the pipeline reacts as an

integrated hydraulic system in which mass imbalance forces a global redistribution of pressure.

Immediately after leakage initiation, the pressure decrease is governed by local mass removal. However, within a short time interval the entire pipeline begins to participate in restoring hydraulic equilibrium. Because flow resistance accumulates along the pipeline length, the system compensates the lost mass through redistribution rather than localized acceleration. This explains why measured transients in practice appear smooth and monotonic rather than oscillatory.

The terrain slope plays a decisive role in this redistribution process. In a horizontal pipeline, the pressure decay remains nearly symmetric relative to the leakage location. When inclination is present, gravitational contribution shifts the hydraulic balance point. The downstream section experiences an effectively larger integrated resistance, and therefore a greater portion of the pressure adjustment occurs there. As a result, monitoring stations located far from the leakage point may record stronger pressure drops than stations located closer to it.

This observation has important diagnostic consequences. Traditional leak detection methods assume that the largest pressure drop occurs near the leakage location. The model demonstrates that this assumption may fail in inclined pipelines. Under certain operating conditions, the outlet pressure can decrease more rapidly than the inlet pressure even when the leak is located upstream. Therefore, spatial pressure gradients alone cannot uniquely identify the leak position.

Instead, the time evolution of pressure contains the diagnostic information. The relative rates of pressure decay at different monitoring locations form a characteristic signature determined by the pair ($\ell$, $G_{ut}$). By fitting the analytical solution to measured pressure histories, the leakage position and its severity can be identified simultaneously. This transforms leak detection from a threshold problem into an inverse transient identification problem.

Another important implication concerns monitoring reliability. Because the disturbance spreads across the full pipeline, single-sensor detection strategies may lead to false localization. A distributed measurement interpretation based on the analytical model is therefore required. The model effectively acts as a physical filter, separating terrain-induced redistribution from actual measurement anomalies.

From an operational standpoint, this explains why SCADA operators sometimes observe pressure decreases at remote stations before confirming abnormalities near the actual defect location. The phenomenon is not a sensor error but a natural consequence of hydraulic balancing in an inclined pipeline.

In summary, the analytical solution provides not only pressure prediction but also a physically interpretable diagnostic framework. Leakage detection becomes a model-based identification process in which pressure evolution patterns serve as system fingerprints rather than simple alarm thresholds.

## 6. Results and discussion

This section presents the spatiotemporal behavior of pressure distribution in a relief-affected gas pipeline system under unsteady flow conditions. The analysis is based on a parametric variation of the terrain slope angle ($\alpha_1$=10°, 20°, 30°, 40°), leakage location along the pipeline ($\ell$=2500 m, 15000 m, 27500 m), and leakage intensity represented by a fixed mass outflow rate $G_{ut}$=2.5 Pa×s/m. The governing pressure equation incorporates terrain-induced gravitational effects and frictional losses via modified coefficients $\lambda_1$ and $\lambda_2$.

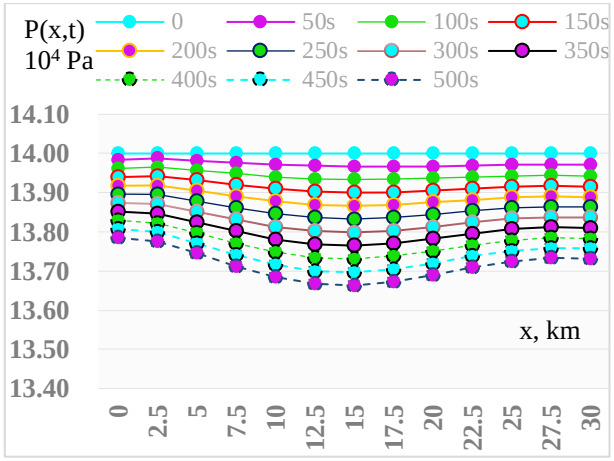


Figure 2.1. Spatiotemporal pressure distribution along a terrain-influenced pipeline ($G_{ut}$=2.5 Pa×s/m, ℓ=2500 m, $\alpha_1$=10°)

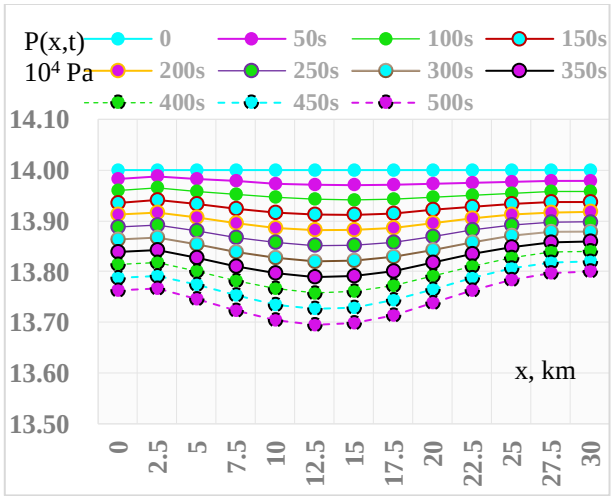


Figure 2.2. Spatiotemporal pressure distribution along a terrain-influenced pipeline ($G_{ut}$=2.5 Pa×s/m, ℓ=2500 m, $\alpha_1$=20°)

## 6.1 Leakage near the inlet (ℓ=2500 m)

Figs. 2.1-2.4 depict the pressure evolution when the leakage occurs near the pipeline inlet.

The following dynamic characteristics are observed:

When the slope angle is relatively small ($\alpha_1 \leq 20°$), the pressure decay at the pipeline outlet exceeds that at the inlet, despite the leakage being near the entry point. This phenomenon contrasts with classical behavior in horizontal pipelines, where inlet-side losses dominate. As the slope increases beyond $20^0$, the pressure gradient reverses: decay near the inlet accelerates, while decay at the outlet becomes milder. This shift is driven by the increasing influence of the gravitational force component $g\sin(\alpha)$, which resists upstream flow and enhances local energy dissipation.

Pressure maxima are observed around:

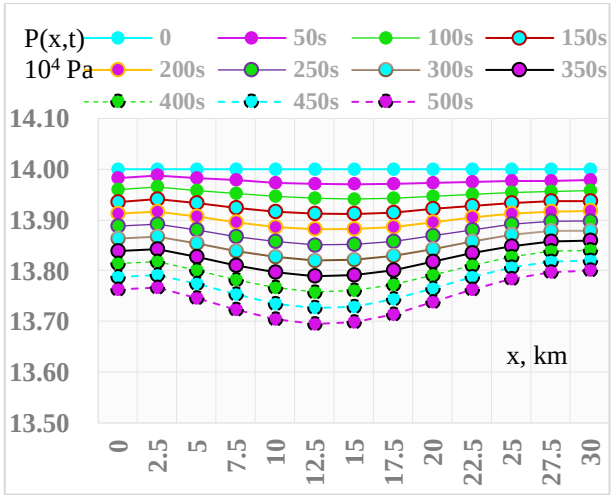


Figure 2.3. Spatiotemporal pressure distribution along a terrain-influenced pipeline ($G_{ut}$=2.5 Pa×s/m, ℓ=2500 m, $\alpha_1$=30°)

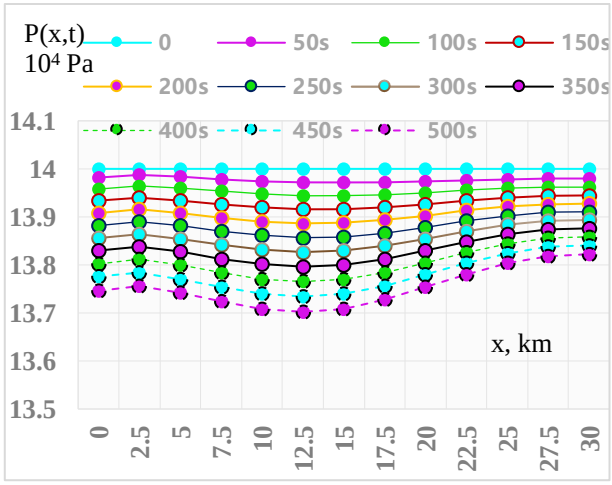


Figure 2.4. Spatiotemporal pressure distribution along a terrain-influenced pipeline ($G_{ut}$=2.5 Pa×s/m, ℓ=2500 m, $\alpha_1$=40°)

x=15 km for $\alpha_1$=10°
x=12.5 km for $\alpha_1 \geq 20°$

These results demonstrate a nonlinear spatial redistribution of pressure peaks influenced by terrain gradient. The pressure drops on both sides of the peak, with stronger decay toward the inlet for higher slopes.

## 6.2 Leakage at the midpoint (ℓ=15000 m)

Figs 3.1-3.4 show the evolution of pressure for leakage at the pipeline midpoint. The key observations are:

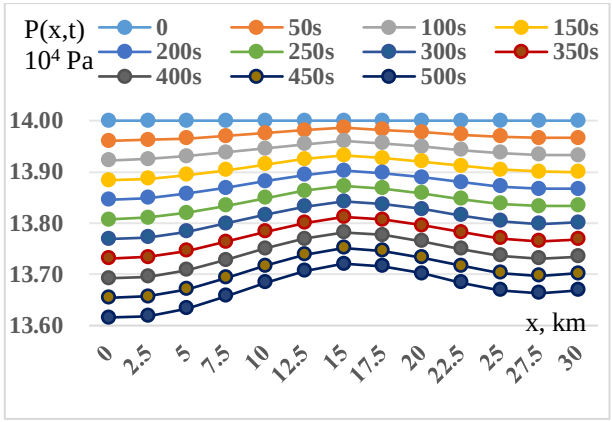


Figure 3.1. Spatiotemporal pressure distribution along a terrain-influenced pipeline ($G_{ut}$=2.5 Pa×s/m, $\ell$=15000 m, $\alpha_1$=10°)

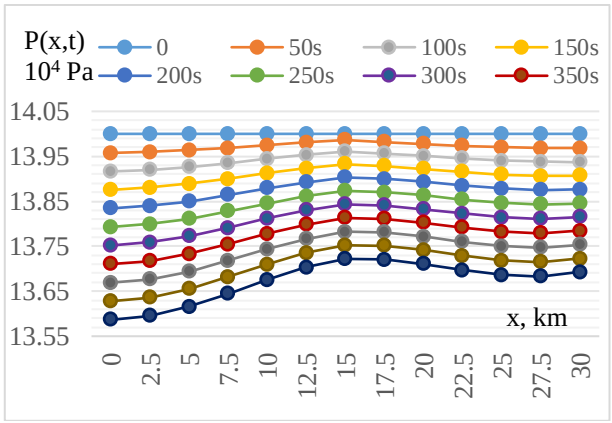


Figure 3.2. Spatiotemporal pressure distribution along a terrain-influenced pipeline ($G_{ut}$=2.5 Pa×s/m, $\ell$=15000 m, $\alpha_1$=20°)

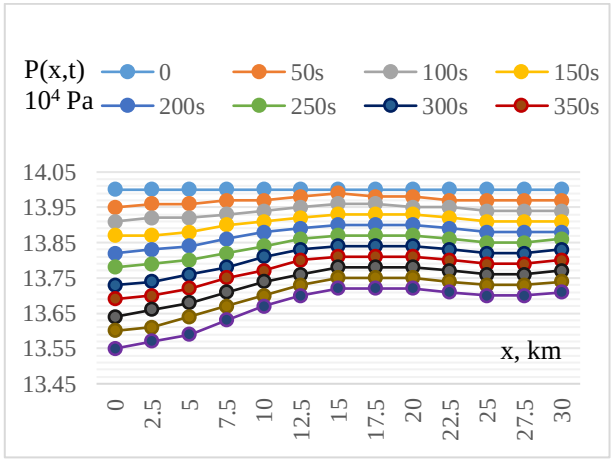


Figure 3.3. Spatiotemporal pressure distribution along a terrain-influenced pipeline ($G_{ut}$=2.5 Pa×s/m, $\ell$=15000 m, $\alpha_1$=30°)

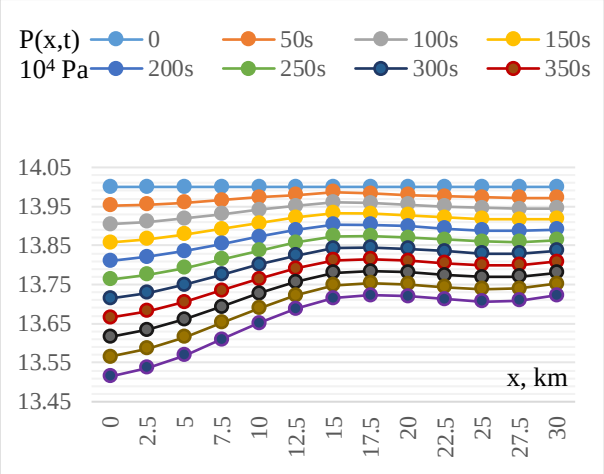


Figure 3.4. Spatiotemporal pressure distribution along a terrain-influenced pipeline ($G_{ut}$=2.5 Pa×s/m , ℓ=15000 m, $\alpha_1$=40°)

The minimum pressure consistently occurs at the leakage location (x=ℓ) and remains nearly constant across all slope angles, demonstrating the localized dominance of $G_{ut}$ in the governing model.

Pressure increases symmetrically in both upstream and downstream directions from the leakage point, though this symmetry degrades as $\alpha_1$ increases.

For higher slope angles, the maximum pressure shifts slightly toward the upstream section, confirming the terrain's asymmetric influence on flow dynamics.

This scenario highlights the importance of nonlinearity in pressure propagation, as governed by the coupled exponential and harmonic terms in the analytical solution. The physical insight is that gravitational opposition upstream increases wavefront resistance, concentrating pressure decay in the inlet segment.

### 6.3 Leakage near the outlet (ℓ=27500 m)

Figs. 4.1-4.4 correspond to leakage near the pipeline outlet.

The results reveal:

Pressure reaches a minimum near the leakage location, and increases toward both ends, albeit with distinct characteristics:

Upstream: Pressure decays from the maximum.

Downstream: Pressure increases, then stabilizes toward the leakage minimum.

As the slope angle increases, the pressure maximum shifts upstream, indicating stronger gravitational influence.

$\alpha_1$=10°→x=15 km

$\alpha_1$=20°→x=12.5 km

$\alpha_1$=30°→x=10 km

$\alpha_1$=40°→x=7.5 km

This consistent upstream migration of the pressure peak illustrates that as slope increases, the zone of highest resistance shifts toward the inlet, significantly altering the transient pressure

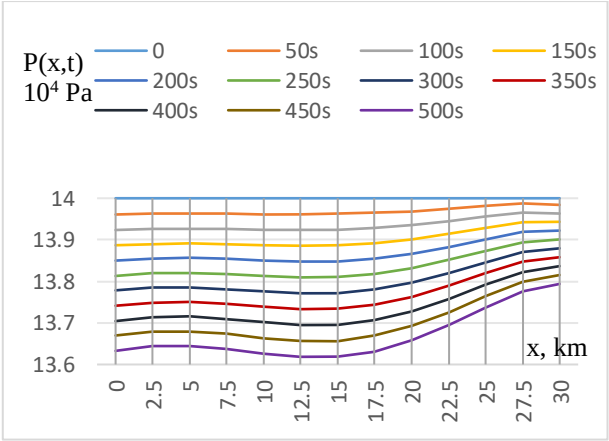


Figure 4.1. Spatiotemporal pressure distribution along a terrain-influenced pipeline ($G_{ut}$=2.5 Pa×s/m, ℓ=27500 m, $\alpha_1$=10°)

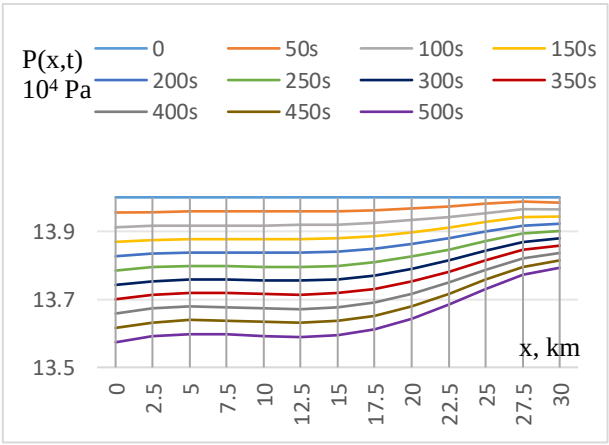


Figure 4.2. Spatiotemporal pressure distribution along a terrain-influenced pipeline ($G_{ut}$=2.5 Pa×s/m, ℓ=27500 m, $\alpha_1$=20°)

landscape. The redistribution of pressure extremes implies that control strategies and sensor placement (e.g., in SCADA or IoT-based monitoring) should be terrain-sensitive.

## 6.4 Pressure-time evolution at key locations

Figs. 5.1 through 5.4 illustrate the temporal evolution of pressure at the inlet (x=0) and outlet (x=L) of the terrain-influenced pipeline for different leakage intensities $G_{ut}$=(2.5, 5.0, 7.5) Pa×s/m and inclination angles $\alpha_1$=(10°, 20°, 30°, 40°), while the leakage is fixed at ℓ=2500 m (i.e., near the inlet section).

The following dynamic patterns and insights were observed:

Symmetry at Low Slope and Leakage Levels:

At $\alpha_1$=10° (Fig. 5.1), and for low leakage intensities (e.g., $G_{ut}$=2.5 Pa×s/m), the pressure drop near the pipeline outlet remains marginally higher than that at the inlet over the simulation period.

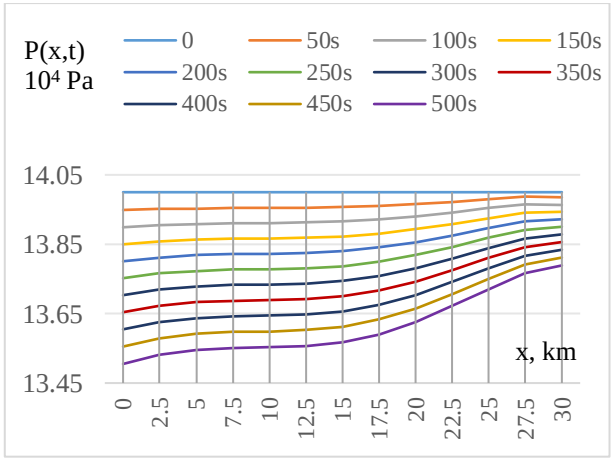


Figure 4.3. Spatiotemporal pressure distribution along a terrain-influenced pipeline ($G_{ut}$=2.5 Pa×s/m, ℓ=27500 m, $\alpha_1$=30°)

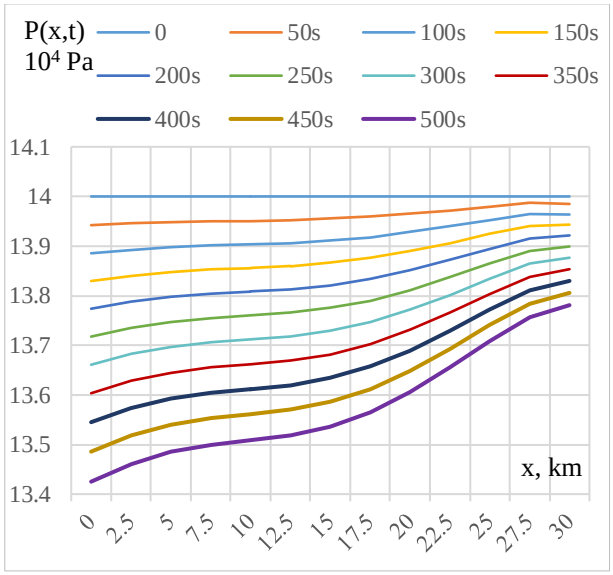


Figure 4.4. Spatiotemporal pressure distribution along a terrain-influenced pipeline ($G_{ut}$=2.5 Pa×s/m, ℓ=27500 m, $\alpha_1$=40°)

This behavior aligns with traditional expfectations for slightly inclined pipelines: the outlet segment, being further downstream, accumulates pressure loss due to friction and elevation. Onset of Pressure Inversion with Increased Leakage:

As $G_{ut}$ increases to 5.0 and 7.5 Pa×s/m, a reversal is observed-particularly after t=150-300 s-where pressure at the inlet drops more rapidly than at the outlet, despite the leakage being closer to the entry point.

This phenomenon is attributed to the localized mass loss near ℓ=2500 m, which depressurizes the upstream segment more directly than the distal outlet. Influence of Terrain Gradient:

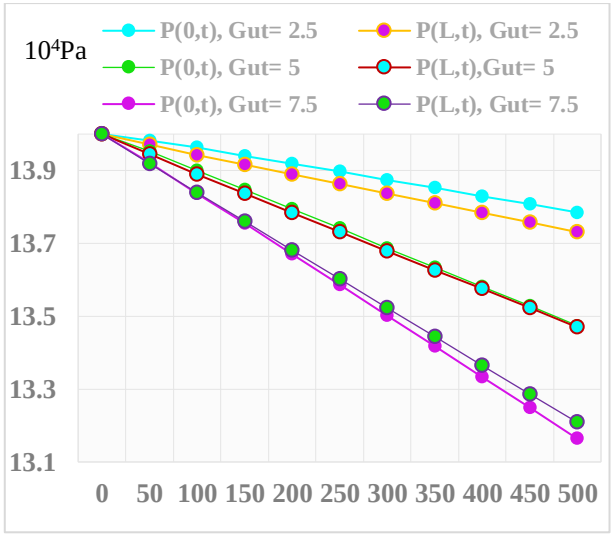


Figure 5.1. Temporal variation of pressure at the inlet and outlet of a terrain-influenced gas pipeline system under different leakage intensities (ℓ=2500 m, $\alpha_1$=10°)

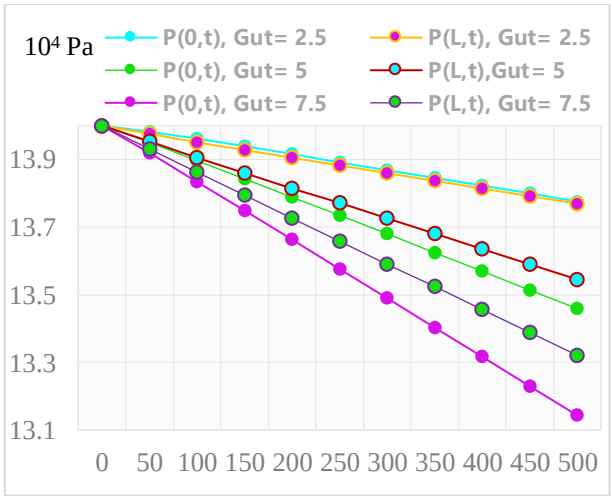


Figure 5.2. Temporal variation of pressure at the inlet and outlet of a terrain-influenced gas pipeline system under different leakage intensities (ℓ=2500 m, $\alpha_1$=20°)

At higher inclination angles (Figs. 5.2-5.4), the gravitationally induced term $\lambda_2 = -\frac{gSin\alpha}{2c^2}$ becomes more pronounced, amplifying asymmetry in pressure distribution. Specifically, for $\alpha_1$=30° and 40°, even under moderate leakage ($G_{ut}$=5.0 Pa×s/m), the outlet pressure remains higher than that at the inlet during extended transient periods, reversing the classical assumption of monotonic decay from inlet to outlet.

Time-Dependent Crossover:

A critical time-dependent crossover was detected: For each increase in $\alpha_1$, the moment at which P(0,t)<P(L,t) occurs earlier in the transient profile.

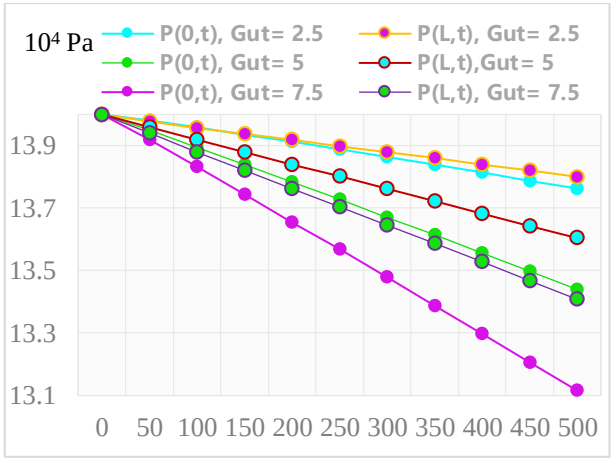


Figure 5.3. Temporal variation of pressure at the inlet and outlet of a terrain-influenced gas pipeline system under different leakage intensities (ℓ=2500 m, $\alpha_1$=30°)

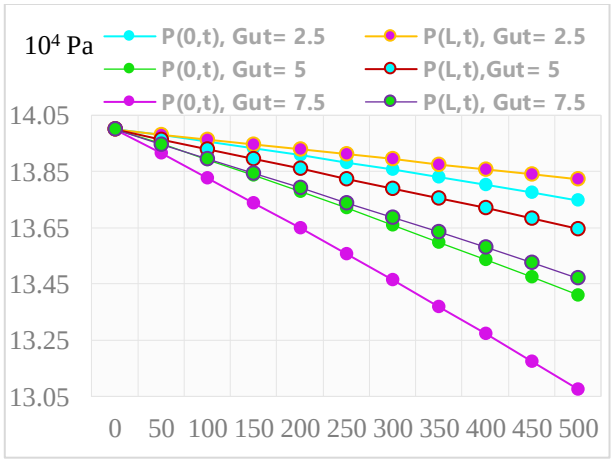


Figure 5.4. Temporal variation of pressure at the inlet and outlet of a terrain-influenced gas pipeline system under different leakage intensities (ℓ=2500 m, $\alpha_1$=40°)

This effect highlights the coupling between gravitational slope and leakage dynamics-where the gravitational potential modulates the effective friction and velocity profile over time.

Quantitative Observations (Excerpts):

At $\alpha_1$=10°, $G_{ut}$=7.5, the pressure at inlet and outlet at t=500 s were $13.16\times10^4$ Pa and $13.21\times10^4$ Pa respectively.

At $\alpha_1$=40°, the same case yielded P(0,t)=$13.08\times10^4$ Pa and P(L,t)=$13.47\times10^4$ Pa, further amplifying the inversion.

Physical and Technological Implications:

Physically, the observed pressure inversion is due to the dominance of terrain-induced forces and the spatial position of the leakage. The gravitational force accelerates gas along the slope, making the downstream sections more stable against pressure loss for upstream leakages.

Technologically, this has significant implications for leak detection algorithms: conventional

models assuming higher pressure loss at the outlet may misinterpret early warning signals or mislocalize the leak origin.

For SCADA systems, the findings suggest the need for terrain-aware calibration models and adaptive sensor deployment strategies that consider slope and leakage coupling.

Operational pressure records in long transmission pipelines rarely contain resolvable acoustic oscillations due to strong frictional damping and low sampling frequency of monitoring systems. The model therefore describes relaxation-type transient redistribution rather than wave propagation, which is consistent with observed field pressure behavior.

## 7. Practical ımplications and future development

The analytical model derived in this study is not limited to theoretical description of pressure redistribution but also provides a practical framework for real-time monitoring and control of gas transmission systems. Modern pipeline operation relies increasingly on SCADA and IoT infrastructures, where decisions must be made using incomplete and noisy measurements. The closed-form nature of the solution enables direct evaluation of transient pressure behavior at any spatial location without iterative numerical solvers, making it suitable for embedded monitoring environments and digital twin platforms.

One of the main operational consequences of the obtained solution is the reinterpretation of pressure measurements during leakage events. Conventional monitoring logic assumes that the largest pressure drop occurs near the defect location. The present results demonstrate that in terrain-influenced pipelines this assumption may be incorrect, since gravitational drift redistributes hydraulic imbalance along the entire pipe. As a result, remote stations may register stronger pressure decay than stations located closer to the leakage point. This explains previously reported inconsistencies in operational diagnostics and supports the need for model-based interpretation rather than threshold-based alarm rules.

The model also provides guidance for sensor deployment strategy. Because diagnostic information is contained in the temporal evolution of pressure rather than instantaneous spatial gradients, optimal monitoring is achieved by distributing a limited number of sensors along hydraulically informative positions instead of concentrating them near expected failure zones. The analytical solution can therefore be used to determine observation points that maximize detectability while minimizing hardware requirements.

From the control perspective, the availability of an analytical transient response allows operators to estimate leakage intensity and position simultaneously by fitting measured pressure histories to the model. This transforms leak management into an inverse identification procedure and enables early decision support, including prioritization of inspection, isolation planning, and risk assessment in inclined terrain conditions.

The structure of the solution also makes it compatible with predictive SCADA algorithms and hybrid data-driven monitoring approaches. Instead of replacing physical modeling, machine-learning classifiers may use the analytical model output as physically consistent features, improving reliability of anomaly detection systems and reducing false alarms caused by terrain-induced pressure redistribution.

Although the present study focuses on a one-dimensional analytical formulation, further development may extend the approach toward experimental validation, networked pipeline configurations, and automated control strategies. Field measurements will allow calibration of

leakage intensity parameters and assessment of measurement uncertainty limits required for reliable detection. In addition, coupling the analytical core with optimization or learning algorithms may enable adaptive regulation of operating regimes in complex pipeline infrastructures.

Overall, the proposed formulation establishes a bridge between theoretical gas dynamics and practical monitoring technology, providing a physically interpretable basis for next-generation intelligent pipeline management systems.

## 8. Conclusions

This study introduces a comprehensive analytical model for simulating unsteady gas dynamics in terrain-influenced pipelines with leakage, incorporating slope-induced gravitational forces and transient gas losses. The derived pressure expression, obtained via Charny linearization and Laplace transformation techniques, provides a closed-form solution that captures the complex interaction between leakage location, terrain gradient, and pressure propagation over time.

The simulation results reveal several critical findings that, to the authors' knowledge, have not been previously reported in the literature or utilized in practical SCADA-based control centers:

Under certain terrain and leakage configurations, the pressure drop at the pipeline outlet may become smaller than that at the inlet-a reversal from classical assumptions-especially when the leakage occurs near the end of the pipeline and slope angle increases.

Terrain inclination significantly affects the temporal stability of pressure dynamics, which may lead to either amplification or damping of leak-induced disturbances, depending on the leak's proximity to high-elevation zones.

The derived model allows early prediction of pressure crossover points, enabling real-time estimation of leak severity and localization with minimal sensor data.

These insights offer novel, theoretically validated information that remains unavailable to current control centers and SCADA platforms without such terrain-aware modeling. Given the increasing integration of IoT-based pressure sensors into modern pipeline infrastructure, the ability to anticipate and interpret such dynamic behaviors is of paramount importance for enhancing reliability, optimizing control strategies, and minimizing safety risks.

Thus, the presented analytical model is not only a scientific advancement in the field of gas dynamics but also serves as a practical decision-support tool for intelligent pipeline management under real-world terrain conditions. The model provides, for the first time, a closed-form solution that captures pressure inversion effects in inclined gas pipelines-an effect critical for modern SCADA diagnostics.

## Highlights

First analytical model for unsteady gas flow in pipelines accounting for terrain slope, gravitational effects, and leakage.

Reveals pressure drop inversion phenomena, previously unknown to traditional SCADA control centers.

Incorporates Charny linearization and Laplace transform for closed-form pressure distribution solutions.

Enables IoT-integrated monitoring and terrain-aware leak localization with minimal sensor data.

Delivers actionable insights for control center decision-making, enhancing safety and energy efficiency.

## References


1. Thorley, A.R.D., Tiley, C.H. (1987). Unsteady and transient flow of compressible fluids in pipelines—A review of theoretical and some experimental studies. International Journal of Heat and Fluid Flow, 8(1), 3-15. https://doi.org/10.1016/0142-727X(87)90044-0.
2. Weymouth, T.R. (1912). Problems in natural gas engineering. Transactions of the American Society of Mechanical Engineers, 34, 185-231. https://doi.org/10.1115/1.4059982.
3. Panhandle Eastern Pipe Line Company (1940). Flow of natural gas through transmission lines. American gas association proceedings.
4. Sundar, K., Zlotnik, A. (2018). State and parameter estimation for natural gas pipeline networks using transient state data. IEEE Transactions on Control Systems Technology, 27(5), 2110-2124. https://doi.org/10.1109/TCST.2018.2851507.
5. Marusak, N., De La Ree, J., Centeno, V. (2018). Pipeline leakage detection using transient modeling and SCADA data analytics. IEEE Transactions on Industry Applications, 54(5), 4743–4750. https://doi.org/10.1109/TIA.2018.2828860.
6. Aliyev, I. (2025). Modeling and analysis methods for early detection of leakage points in gas transmission systems. arXiv preprint arXiv:2504.06809. https://doi.org/10.48550/arXiv.2504.06809.
7. Wang, J., Li, C., Chen, C., Jia, W. (2025). A CFD study of the unsteady leakage and dispersion of natural gas pipelines containing high-$H_2S$ in mountainous terrain. Process Safety and Environmental Protection, 197, 106981. https://doi.org/10.1016/j.psep.
8. Xu, D., Chen, L., Zhan, W., Zhang, K., Lu, J., Ji, Y., Ma, R. (2023). Study on the leakage dispersion law of exposed high-pressure natural gas pipelines in the mountainous environment. Frontiers in Energy Research, 10, 1031006. https://doi.org/10.3389/fenrg.2022.1031006.
9. Kim, J., Han, S., Kim, D., Lee, Y. (2024). Gas pipeline leak detection by integrating dynamic modeling and machine learning under transient state. Energies, 17(21), 5517. https://doi.org/10.3390/en17215517.
10. Du, J., Li, H., Liao, Q., Shen, J., Zheng, J., Liang, Y. (2024). A knowledge-inspired hierarchical physics-informed neural network for pipeline hydraulic transient simulation. arXiv preprint arXiv:2409.10911. https://doi.org/10.48550/arXiv.2409.10911.
11. Li, M., Zhang, Y., Wang, C., Li, X. (2021). Simulation of gas pipeline flow under elevation changes using improved finite difference methods. Journal of Natural Gas Science and Engineering, 92, 103987. https://doi.org/10.1016/j.jngse.2021.103987.
12. Quintela, P., Pérez Parra, J.C., Useche Castro, L., Lapo Palacios, M. (2020). Simulation of transient flow in gas pipelines using the finite volume method. Revista Científica y Tecnológica UPSE (RCTU), 7, 17-26. https://doi.org/10.26423/rctu.v7i2.534.
13. Pashali, A.A. (2019). Modeling the conditions for generating liquid plugs by a relief pipeline profile. Territory Neftegaz, 5, 68-74.
14. Izotova, E.A., Fominykh, G.S. (2021). Analysis of engineering solutions in the construction of gas pipelines in difficult conditions. Technical Regulation in Transport Construction, 4(49), 171-178.